Available online at www.sciencedirect.com
ScienceDirect
Journal of the European Ceramic Society 27 (2007) 1767–1773
www.elsevier.com/locate/jeurceramsoc

Measurement of Vickers hardness on ceramic floor tiles

Leposava Sidjanin [a,*], Dragan Rajnovic [a], Jonjaua Ranogajec [b], Elvira Molnar [b]

[a] Department for Production Engineering, Faculty of Technical Sciences, University of Novi Sad, Trg D. Odradovica 6, 21000 Novi Sad, Serbia and Montenegro
[b] Department of Materials Engineering, Faculty of Technology, University of Novi Sad, Bul. Cara Lazara 1, 21000 Novi Sad, Serbia and Montenegro

Available online 6 June 2006

Abstract

In this paper, Vickers macro- and micro-hardness of ceramic floor tiles samples made from two types of clay materials, kaolinite and illite–carbonate raw materials, were presented. The samples, designed separately, from both types of clay materials were shaped by dry pressing at 25 MPa, then fired at 960 and 1050 °C in laboratory conditions and exposed to freezing/thawing cycles with the aim to compare the hardness before and after cycling and correlate it to their microstructure. The results showed that Vickers macrohardness increases with the increasing of the firing temperature, although the expected microstructure is not achieved. The results obtained after freezing and thawing follow the same trend. In addition, the indentation size effect (ISE) in the case of low-load hardness testing was analysed. It should be noticed that the samples based on illite–carbonate clay material after the freezing/thawing cycles showed an unexpected increasing of hardness. The obtained results might be the consequence of the calcium silica hydrates formation during cycling treatment, causing a different behaviour of this kind of systems under low-loading. The ISE was described through the application of the Mayer's law, proportional specimen resistance (PSR) model and modified PSR model. The best correlation between measured values and used models was achieved in the case of modified PSR model. The most reliable results for the load independent hardness, H_{LIH}, were obtained in the case of Vickers hardness measurement HV1.

Keywords: Traditional ceramics; Firing; Microstructure-final; Hardness; Frost resistance

1. Introduction

Hardness testing is the most frequently used method for characterizing mechanical properties of ceramics. An indenter of well-defined geometry is pressed into the surface of the sample under a predefined load.[1] The quotient of the load and the area of the residual indentation impression are regarded as the measure of hardness. Three levels of indentation hardness are measured: the nano, the micro and macro.[2] Nanohardness indentations are on the sub-micron scale and can be used to estimate the mechanical properties of very fine structures including precipitates and thin films.[3] The microhardness indentations are of the micron size scale and have been extensively applied at the microstructure level when Vickers diamond pyramid indenters are usually applied.[4] Macrohardness measurements are much larger in scale then micro- and nano-hardness and are often applied as bulk testing procedures. However, when macrohardness measurements are applied to ceramics, the testing usually results in chipping and formation of massive cracks.[5] In contrast, when microhardness testing is applied, the measured values of hardness decrease with the increasing test load, showing the "indentation size effect" (ISE).[6]

The existence of the ISE implies absence of a single value for the microhardness. At high indentation test loads, the microhardness is constant as far as the indentation test load and a single hardness value are concerned, a phenomenon described as the load independent of hardness, H_{LIH}, or the "true" hardness.[2] In this paper, Vickers macro- and micro-hardness of two types of ceramics floor tiles were presented. The samples belong to the model systems based on kaolinite/illite–carbonate composition. In addition, the ISE for the low-load hardness testing of the model system specimens was analysed. The ISE reported here was described quantitatively through the application of the Mayer's law, proportional specimen resistance (PSR) model and modified PSR model[7–10] to best correlate measured values with mathematical models.

2. Experimental procedure

The cross-section of a ceramic floor tile is given on Fig. 1. The tile consists of three layers: glaze on the top, engobe in the middle and biscuit as a ceramic matrix.

* Corresponding author. Tel.: +381 21 450366; fax: +381 21 454495.
E-mail address: lepas@uns.ns.ac.yu (L. Sidjanin).

0955-2219/$ – see front matter © 2006 Elsevier Ltd. All rights reserved.
doi:10.1016/j.jeurceramsoc.2006.04.150

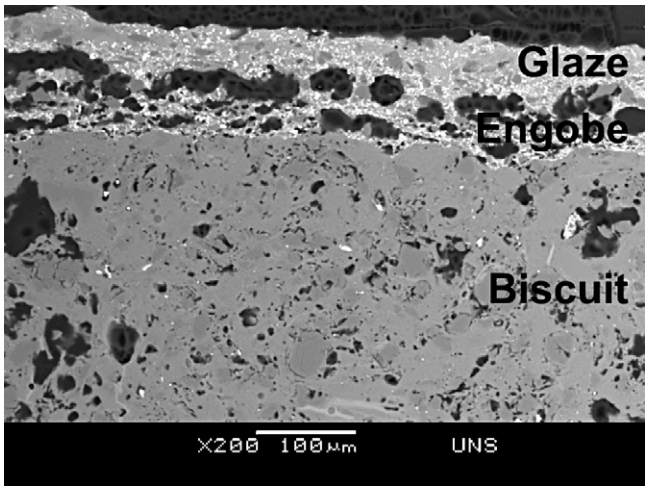

Fig. 1. The cross-section of the floor tile, SEM image.

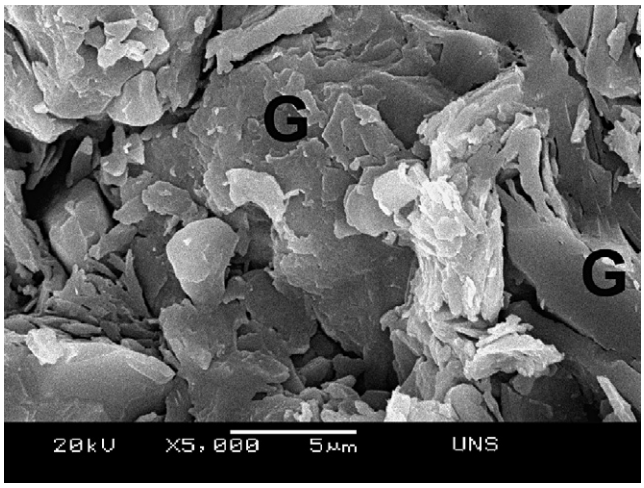

Fig. 2. SEM image of the K sample system fired at 1050 °C-before freezing/thawing procedure, (G—amorphous/glassy phase).

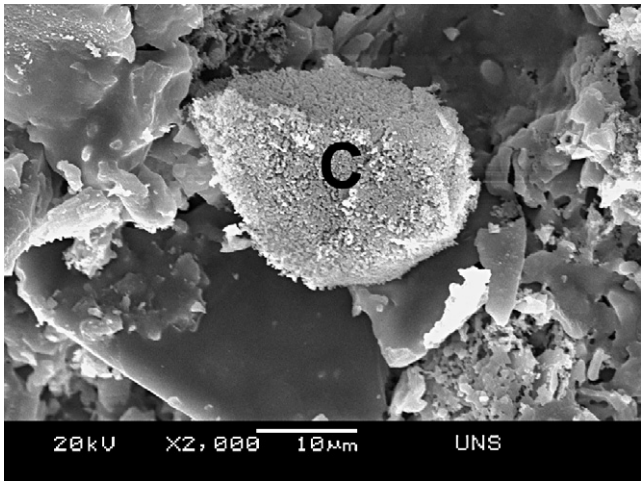

Fig. 3. SEM image of the IC sample system fired at 1050 °C-before freezing/thawing procedure, (C—unreacted free CaO).

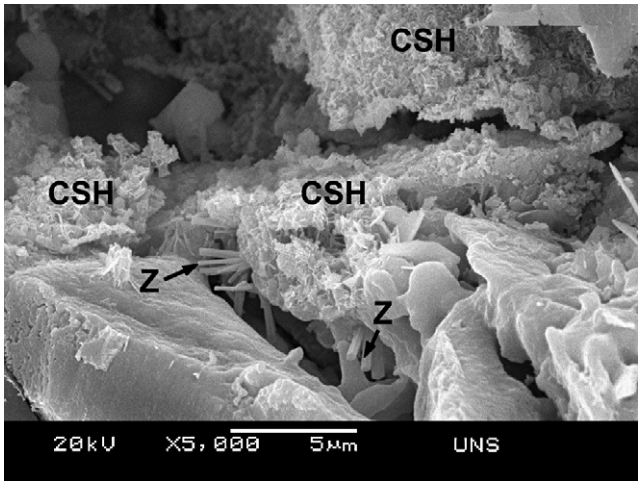

Fig. 4. SEM image of the IC sample system fired at 960 °C-after freezing/thawing procedure, (Z—zeolite crystals and CSH—calcium silicate hydrates).

In this study, two model systems, formed from different types of raw materials, (ceramic matrix), were used. One raw material was a mixture of kaolinite, quartz and plagioclase (K system: $Al_2O_3/SiO_2 = 17.61/71.61$; MgO = 0.80 mass%; $K_2O = 2.42$ mass% and $Na_2O = 0.30$ mass%), while the other contained illite, quartz and carbonates (IC system: $Al_2O_3/SiO_2 = 9.88/47.83$; CaO = 13.73 mass%). The values of the moisture level of the initial raw materials were different. For the K model it was 1.17 mass%, while for the IC it was 2.12 mass%. The specimens were shaped by dry pressing at 25 MPa to a size of 5 mm × 5 mm × 25 mm. After shaping procedure the samples were fired at 960 and 1050 °C. The soaking time at each maximum temperature was 90 min. Furthermore, half of the specimens were exposed to the standard frost resistant procedure (EN 539-2). The idea was to compare their hardness values before and after the standard procedure of freezing/thawing.

Vickers hardness measurements HV0.1, HV0.2, HV0.5, HV1 and HV5, were performed according to ISO 6507, using indentation loads: 0.9807 N (0.1 kgf), 1.961 N (0.2 kgf), 4.903 N (0.5 kgf), 9.807 N (1 kgf) and 49.03 N (5 kgf), respectively. Indentation tests were carried under laboratory conditions on Highwood HW DW-3 Vickers tester with error of measurement ±0.1 μm. Before hardness measurements all specimens were prepared by the standard metallographic technique.[6] The samples were mounted with epoxy resin, grinded with SiC papers from grade 220–2400 and than polished up to 0.25 μm with a diamond paste and finally coated with gold in a vacuum. Their reflectivity was improved in order to precisely measure the length of the two diagonals of the square-shaped Vickers indentation (Leitz light microscope with a magnification of 200×). Microstructural features were examined using a scanning electron microscope (JEOL JSM 6460LV).

3. Results and discussion

3.1. Microstructure characteristics

3.1.1. State before the freezing procedure

The kaolinite system (K system), due to the absence of carbonates and thermal transformations within Al_2O_3–SiO_2 com-

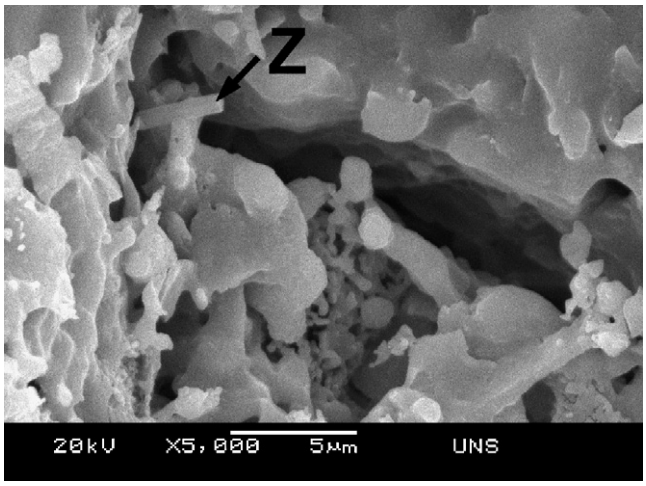

Fig. 5. SEM image of the IC sample system fired at 1050 °C-after freezing/thawing procedure, (Z—zeolite crystals).

position, in the presence of K/Mg ions, contains a considerable amount of amorphous/glassy phase, Fig. 2. The mechanical properties of this system were improved by intercalation of quartz and crystobalite crystals and by the existence of sealed porosity. On the other hand, the illite–carbonate system (IC system), due to the high carbonate content and insufficient quantity of clay minerals necessary for the formation of Ca/Al silicates, possesses unreacted free CaO, Fig. 3. The presence of free CaO makes this system less meltable and the CO_2 release increases its porosity.[11–13] Moreover, slight forces kept the layers of illite clay mineral together after the thermal treatment.[14] Therefore, those facts indicated that mechanical properties of the IC samples might decrease.

Table 1
Vickers hardness

System	HV5 (MPa)	
	Not cycled	Cycled
K960	381	115
K1050	1115	644
IC960	225	115
IC1050	272	196

3.1.2. State after the freezing procedure

The bar shaped crystals were noticed at the end of the standard freezing procedure for the IC system, fired at 960 °C. Zeolite crystals and calcium silicate hydrates were identified, Fig. 4. However, fired at 1050 °C the IC system showed only zeolite crystals, Fig. 5. The analysis of the microstructure of the both K systems, showed no appearance of new crystal formations. These results suggest that the frost actions changed only the pore structure in the samples of K system without revealing new crystal forms during freezing procedure.

3.2. Vickers hardness

3.2.1. Macrohardness

The macro Vickers hardness values HV5 for all used specimens are given in Table 1. The results show that the maximum

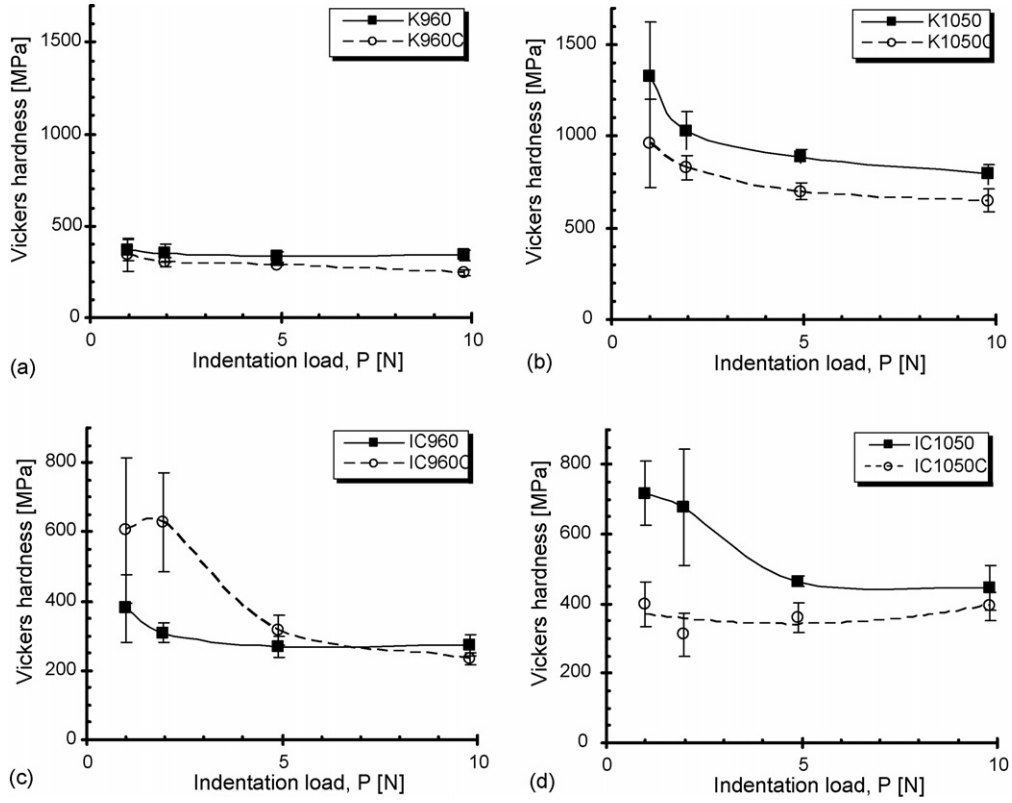

Fig. 6. Vickers hardness obtained by low-loading: (a and b) K system; (c and d) IC system.

hardness value was obtained for the not cycled K 1050 specimen. The results also show that the increase of firing temperatures lead to the increase of hardness, where the hardness for the K specimens were always higher. These results correlate well with the specimens microstructure. The observed carbonate content (greater than 10%) appears to make the system less meltable and more porous. Even slight forces, which keep the layers of illite clay mineral together, cause the IC specimens to have lower hardness than specimens of the K systems. In contrast, the absence of carbonate and thermal transformations within Al_2O_3–SiO_2 composition, cause the formation of a considerable amount of amorphous/glassy phase and sealed porosity. Consequently, these conditions cause higher values of hardness in the case of model samples K in comparison with the IC model systems. The results after 35 cycles of freezing follow the same pattern as non-cycled samples. For the K system the values of hardness remained greater following freezing and thawing procedures. For each firing temperature, hardness value of both, K and IC samples, were smaller compared to that of non-cycled samples. The drop of hardness after cycling is likely due to the micro cracks formation, as the consequence of frost sample damage.

3.2.2. Microhardness

The Vickers hardness numbers obtained by loading with 0.9807, 1.961, 4.903, 9.807 N, for the model system of two types of clay materials and two types of firing temperature used, before and after cycling, are plotted in Fig. 6(a)–(d) as the functions of the applied test load. Data points represent an average measurement from at least three tests. The ISE was observed in the both, K and IC tile materials. The higher the firing temperature, the higher the hardness values. Hardness after cycling follow the same pattern, but the values are lower compared to the same values before cycling. However, the cycled IC samples, fired at 960 °C, compared with K system, showed an unexpected increasing of the hardness values. These results might be due to the calcium silica hydrate formation during cycling treatment resulting in a different behaviour of the IC samples under low-loading (see Figs. 4 and 6(c)).

Table 2
Regression analysis results of the experimental data according to Meyer's law

System	A	$\log A$	n	Correlation factor (R^2)
K960	159.7	2.203	1.9219	0.9995
K960C	99.4	1.997	1.7668	0.9990
K1050	213.2	2.329	1.6434	0.9987
K1050C	203.6	2.309	1.7064	0.9997
IC960	98.2	1.992	1.7410	0.9967
IC960C	56.1	1.749	1.3574	0.9893
IC1050	125.1	2.097	1.6133	0.9967
IC1050C	197.1	2.295	2.0023	0.9871

The load-dependence of the measured Vickers hardness values can also be described quantitatively through the application of the classical Meyer's law:

$$P = Ad^n \quad (1)$$

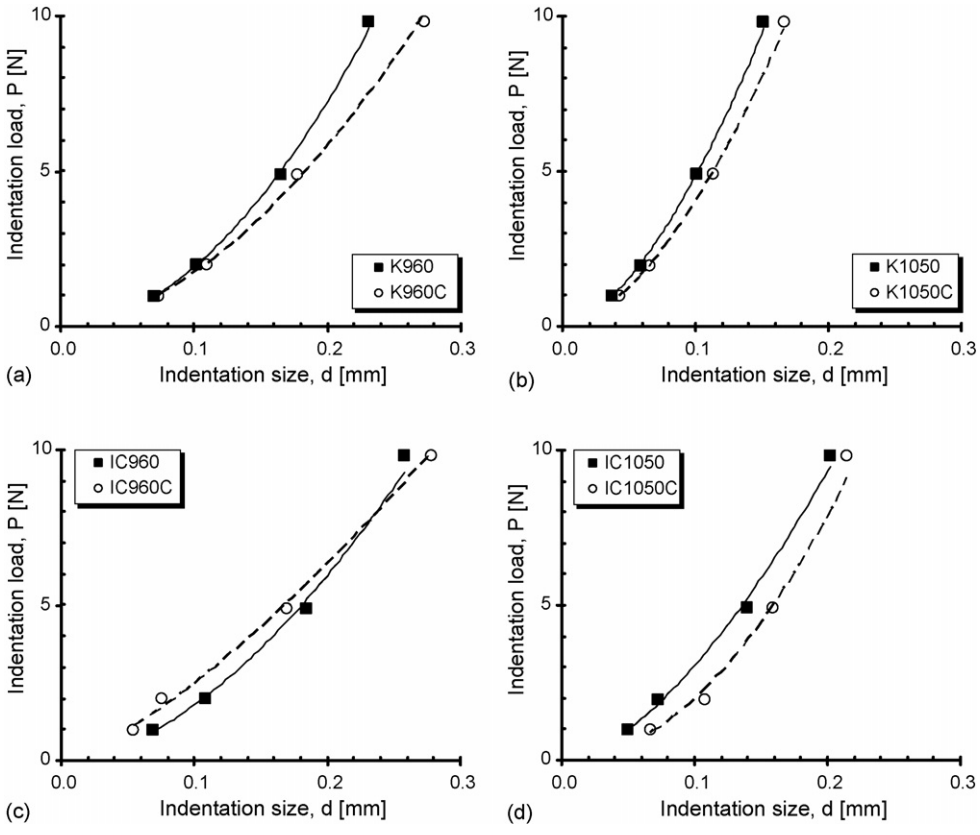

Fig. 7. Correlation between P and d according to the Meyer's law: (a and b) K system; (c and d) IC system.

where P is the indentation test load and d is the resulting indentation size. The parameters A and n are values that can be derived directly from the curve fitting of the experimental data. The Meyer's law parameters determined by the regression analyses are summarizes in Table 2 and presented in Fig. 7(a)–(d). The ISE is commonly related to the deviation of the n-value from two. For virtually all materials the power law exponent n is experimentally observed to be between 1 and 2, which indicates that lower indentation test loads result in higher apparent microhardness. The results presented in Table 2 indicated that the most significant ISE was obtained in the case of cycling IC specimens fired at 960 °C ($n = 1.3574$), while the ISE observed in cycling specimens fired at 1050 °C was independent ($n = 2.00$). The correlation factors R^2 are between 0.9893 and 0.9997.

An alternative analysis of ISE to the Meyer's law is proportional specimen resistance (PSR) model based on the Eq. (2)[7]:

$$P = a_1 d + a_2 d^2 \tag{2}$$

and modified from PSR model proposed by Gong et al.,[9] giving:

$$P = P_0 + a_1 d + a_2 d^2 \tag{3}$$

where P_0, a_1, and a_2 are experimental constants.

Eq. (2) means the applicability of the PSR model in order to describe the observed ISE by testing the linearity between P/d and d. Thus, the result is summarized in Table 3 and presented in Fig. 8(a)–(d). From Fig. 8 it is evident that in each system, the data points show linearity with correlation factor R^2 between 0.8610 and 0.9998. The proportional specimen resistance (PSR) model actually was introduced by Li and Bradt.[7]

Table 3
Regression analysis results of the experimental data according to PSR model

System	a_1	a_2	Correlation factor (R^2)
K960	1.437	174.83	0.9981
K960C	5.624	114.14	0.9867
K1050	13.614	338.58	0.9989
K1050C	10.100	289.99	0.9998
IC960	4.729	125.84	0.9906
IC960C	17.467	65.42	0.8610
IC1050	11.520	179.77	0.9812
IC1050C	−2.473	216.20	0.9711

They accepted the concept of the existence of a minimum level of the applied test load. They named it the test of specimen resistance ($W = a_1 d$). Below the minimum level, the permanent deformation, due to the indentation, is not initiated but only elastic deformation occurs.

Eq. (3) is a modified form of the PSR model with the same physical meaning of the parameters a_1 and a_2, as those in Eq. (2). The modified PSR model was suggested by Gong et al.,[9] who found that surface of specimen is not in stress free state, but rather exposed to the same kind of stress induced during machining and polishing of the sample. This stress changes the specimens resistance parameter to ($W = P_0 + a_1 d$), where P_0 is related to the residual surface stresses with small negative value and a_1 with positive value, as they represent a specimen resistance to permanent deformation. The fit values of all parameters included in Eq. (3) for the specimens of K and IC systems are listed in Table 4 and presented in Fig. 9(a)–(d). The solid and dashed lines in the plots

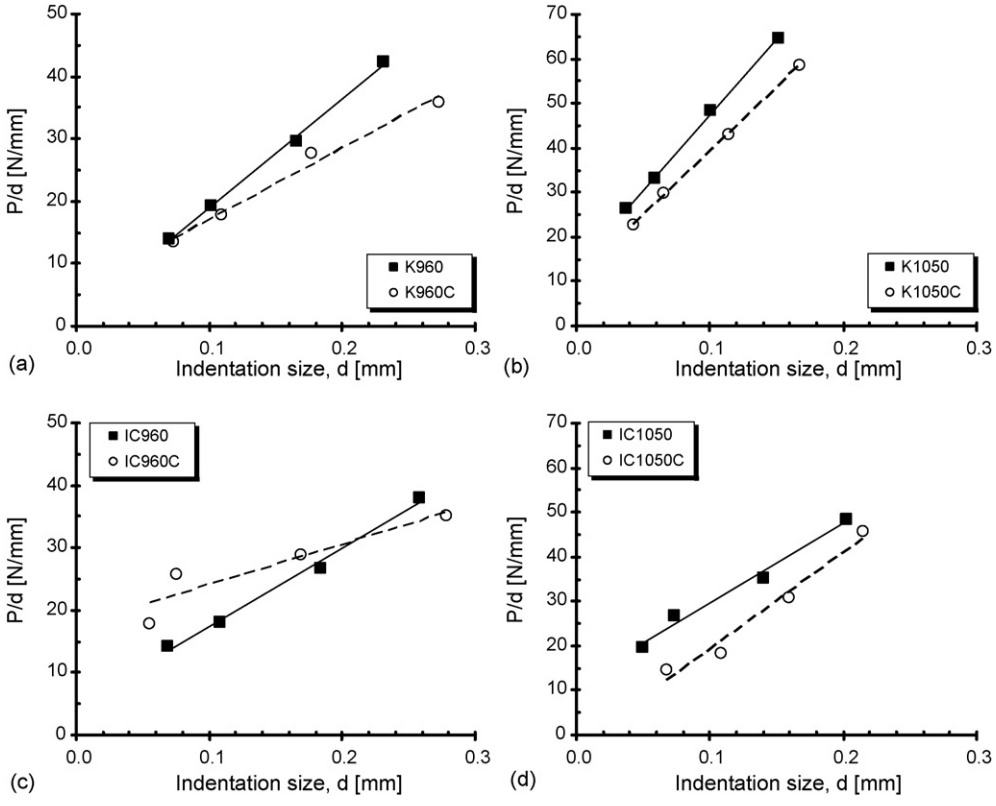

Fig. 8. Correlation between P/d and d: (a and b) K system; (c and d) IC system.

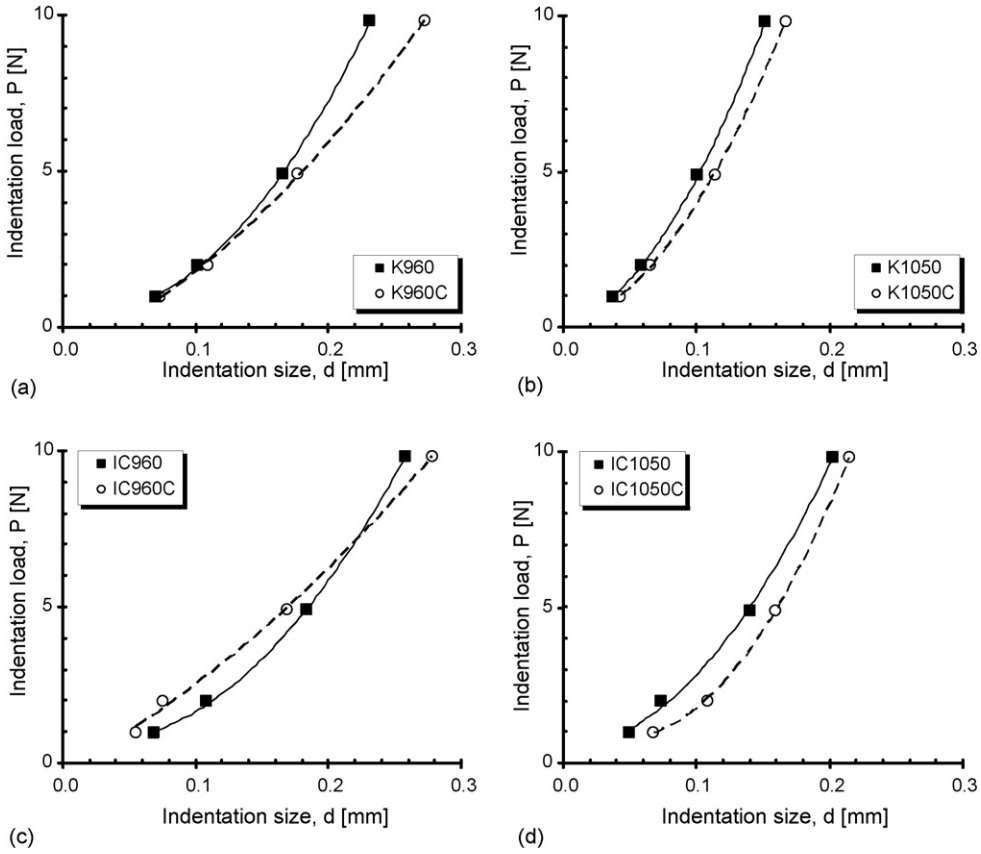

Fig. 9. Correlation between indentation load (P) and size (d): (a and b) K system; (c and d) IC system.

are obtained by conventional polynomial regression according to Eq. (3). For the same Vickers hardness values, the regression analysis returns correlation coefficients between 0.9984 and 1. However, from Table 4 it can be seen that for the same samples the parameter P_0 has a positive value and a_1 negative. The similar results on traditional ceramics were also obtained by Kim and Kim.[6] Very recently, Gong and co-workers,[6,9,15] has given a reasonable explanation for the modified PSR model, based on the consideration of the effect of the porosity of material on the negative or positive values of P_0 and a_1 parameters.

In this paper the results obtained under low-load testing hardness provide the best correlation between measured values and the modified PSR mathematical model. It was also noticed, that the most reliable results for the load independent hardness, H_{LIH} for tiles examined were achieved in the case of Vickers hardness measurement HV1.

Table 4
Regression analysis results of the experimental data according to modified PSR model

System	P_0	a_1	a_2	Correlation factor (R^2)
K960	0.4631	−6.316	201.41	0.9999
K960C	−0.8510	18.554	75.36	0.9993
K1050	−0.0838	15.927	326.19	0.9999
K1050C	0.0226	9.576	292.42	1.0000
IC960	0.7843	−8.026	166.60	0.9997
IC960C	−0.2490	22.611	48.20	0.9984
IC1050	0.4580	1.800	219.20	0.9986
IC1050C	1.4500	−28.469	312.85	0.9998

4. Conclusions

The hardness values of the floor tiles presented in this paper are directly connected to their microstructures which vary according to the mineral composition of the ceramic raw material and the firing temperature. With the increasing of the firing temperature, an increase of hardness values HV5 were observed. The results obtained after cycling follow the same pattern, but the values of hardness were lower compared to the same values before cycling. This was due to the occurrence of micro cracks produced by frost damages. In addition to macrohardness, the indentation size effect ISE obtained under low-load testing, was examined. For ISE the best correlation between measured values and mathematical models was achieved with the modified PSR model. It was also noticed, that the most reliable results of the load independent hardness, H_{LIH}, for the tiles examined were achieved in the case of Vickers hardness measurement HV1.

Acknowledgments

This work was supported through technology development project TR-6735B by Ministry of Sciences and Environmental Protection, Republic of Serbia.

The Vickers hardness measurements were performed in the lab of Department of Mining and Materials Engineering, Prince of Songkla University, Thailand.

References

1. Quinn, G. D., Hardness testing of ceramics. *Adv. Mater. Process.*, 1998, **8**, 23–27.
2. Stevenson, M. E., Kaji, M. and Bradt, R. C., Microhardness anisotropy and the indentation size effect on the basal plane of single crystal hematite. *J. Eur. Ceram. Soc.*, 2002, **22**, 1137–1148.
3. Nagy, P. M., Characterisation of layered materials by combined nanoindentation and AFM. *Microsc. Anal.*, 2004, **18**(6), 13–15.
4. Ullner, C., Germak, A., Doussal, H. L., Morrell, R., Reich, T. and Vandermeulen, W., Hardness testing on advanced technical ceramics. *J. Eur. Ceram. Soc.*, 2002, **22**, 1427–1445.
5. Quinn, G. D., *Indentation Hardness Testing of Ceramics*. *ASM Handbook*, *Vol. 8*, *Mechanical Testing and Evaluation*. Materials Park, Ohio, 2000, pp. 244–251.
6. Kim, H. and Kim, T., Measurement of hardness on traditional ceramics. *J. Eur. Ceram. Soc.*, 2002, **22**, 1437–1445.
7. Li, H. and Bradt, R. C., The microhardness indentation load/size effect in rutile and cassiterite single crystals. *J. Mater. Sci.*, 1993, **28**, 917–926.
8. Li, H., Ghosh, A., Han, Y. H. and Bradt, R. C., The frictional component of the indentation size effect in low load microhardness testing. *J. Mater. Res.*, 1993, **8**(5), 1028–1032.
9. Gong, J., Wu, J. and Guan, Z., Examination of the indentation size effect in low-load Vickers Hardness testing of ceramics. *J. Eur. Ceram. Soc.*, 1999, **19**, 2625–2631.
10. Gong, J. and Li, Y., An energy-balance analysis for the size effect in low-load hardness testing. *J. Mater. Sci.*, 2000, **35**, 209–213.
11. Hip, B. B., Domonkos, K. A., Kilibarda-Sapotic, R., Ranogajec, J. and Marinkovic-Neducin, R., In *Proceedings of the 7th ECERS on Design of Green and Fired Microstructure of Wall Tiles, Part 3*, 2002, pp. 1783–1786.
12. Cultrone, G., Sebastian, E., Elert, K., Torre, M. J., Cayalla, O. and Rodriguez-Navarro, C., Influence of mineralogy and firing temperature on the porosity of bricks. *J. Eur. Ceram. Soc.*, 2004, **24**(3), 547–564.
13. Ikeda, K., Kim, H.-S., Kaizu, K. and Higashi, A., Influence of firing temperature on frost resistance of roofing tiles. *J. Eur. Ceram. Soc.*, 2004, **24**, 3671–3677.
14. Jordan, M. M., Boix, A., Sanfeliu, T. and de la Fuente, C., Firing transformations of cretaceous clays used in the manufacturing of ceramic tiles. *Appl. Clay Sci.*, 1999, **14**, 225–234.
15. Gong, J., Comment on measurement of hardness on traditional ceramics. *J. Eur. Ceram. Soc.*, 2003, **23**, 1769–1772.